Destabilization patterns in chains of coupled oscillators

Serhiy Yanchuk[1,2,3] and Matthias Wolfrum[1]
[1]*Weierstrass Institute for Applied Analysis and Stochastics, Mohrenstrasse 39, 10117 Berlin, Germany*
[2]*Humboldt University of Berlin, Unter den Linden 6, 10099 Berlin, Germany*
[3]*Institute of Mathematics, National Academy of Sciences of Ukraine, Tereshchenkivska 3, 01060 Kiev, Ukraine*
(Received 2 March 2007; revised manuscript received 16 November 2007; published 15 February 2008)

We describe the mechanism of destabilization in a chain of identical coupled oscillators. Along with the transition from stationary to oscillatory behavior of the single oscillator, the network undergoes a complicated bifurcation scenario including the coexistence of multiple periodic orbits with different frequencies, spatial patterns, and modulation instabilities. This scenario, which is similar to the well-known Eckhaus scenario in spatially extended systems, occurs here also in the case of purely convective unidirectional coupling, and hence it cannot be explained as a simple discretization of its spatially continuous counterpart. Although the number of coexisting periodic orbits grows with the number of oscillators, we are able to treat this problem independently of the actual size of the network by investigating the limiting equations for the related spectral problems.

DOI: 10.1103/PhysRevE.77.026212 PACS number(s): 05.45.Xt, 02.30.Oz, 82.40.Ck, 89.75.Hc

I. INTRODUCTION

Networks of coupled oscillators have received significant attention over the last decade [1]. Their study can contribute to the understanding of fundamental dynamical features in coupled systems of many kinds, ranging from atoms or neurons to lasers and living organisms [2,3]. The central question is to understand how specific properties of the individual behavior and the coupling architecture can give rise to the emergence of new collective phenomena. Synchronization and desynchronization are examples of such collective phenomena, which have been extensively investigated (see Ref. [4] and references therein). A particularly challenging task is to deal with networks containing a large number of oscillators [5–13]. Because of the large system size, their treatment is often more complicated and requires different techniques compared with small networks of coupled systems [3,4,14–17]. Examples of some important differences are the characterization of the spectrum [6,10], specific numerical methods [7], different types of instabilities [12] and dynamical regimes [13], and usually a high degree of multistability [9,11] in large networks. As in the well-known Kuramoto system [18], a description of the behavior of a large network has to be based on structural properties of the network that are independent of the actual size.

In this paper, we analyze the destabilization scenario in large networks of identical oscillators where the network has a ring structure, i.e., a linear chain with periodic boundary conditions. Such systems are relevant for many practical systems (see, e.g., Refs. [19,20]), and have attracted a lot of attention in the past [21–25]. As a paradigm for such systems, we investigate in detail a ring of unidirectionally coupled dissipative Stuart-Landau oscillators [26]. We reduce the stability analysis of the large coupled system to the level of complexity of one single oscillator, similarly to the master stability function approach of Pecora and Carroll [27]. In contrast to the approach of Pecora and Carroll, we not only determine the stability boundary, but describe the whole bifurcation scenario. Moreover, we are able to do that while passing to the limit of the number of oscillators tending to infinity. It turns out that in a large lattice an oscillatory instability of an individual oscillator induces a destabilization of the whole network, leading to the emergence of a large number of coexisting periodic solutions with different frequencies, spatial patterns, and stability properties.

We show that the observed bifurcation mechanism is similar to the Eckhaus scenario in spatially extended systems with diffusion [28], where in a similar way a spatially homogeneous stationary state becomes unstable with respect to a growing band of spatial wave numbers, resulting in a band of coexistent Turing patterns. This is remarkable because the resulting spatiotemporal patterns cannot be interpreted as a discretization of well-known effects in partial differential equation (PDE) systems with a continuous spatial variable. Instead, the destabilization patterns are of a genuinely discrete nature and are shown to occur even in systems with purely convective (unidirectional) coupling where corresponding continuous-space systems do not exhibit a similar behavior. Our approach is based on the investigation of the structure of the spectrum of the linearized system in the limit of a large number of oscillators, providing a simple criterion for the observed bifurcation scenario. Based on this observation, our example of the Stuart-Landau oscillators is generic in the sense that the observed phenomenon can be expected in a large class of coupled systems of identical oscillators, provided that the corresponding spectral conditions are met.

II. STABILITY ANALYSIS FOR A LATTICE WITH A ROTATION-INVARIANT STRUCTURE

A general oscillator lattice with a rotation-symmetric structure [see, for example, Figs. 1(a) and 1(d)] can be written as follows:

$$\dot{u}_j = Au_j + \sum_m B_m u_{j+m} + H_j(\mathbf{u}), \tag{1}$$

with the oscillator number $j=1,\ldots,N$ and numbers of coupled modes m taken modulo N. Here, $\mathbf{u}=(u_1,\ldots,u_N)^T$, and $u_j \in \mathbf{R}^n$ represents the state variables of the jth oscillator with a steady state at the origin. The linear terms are sepa-

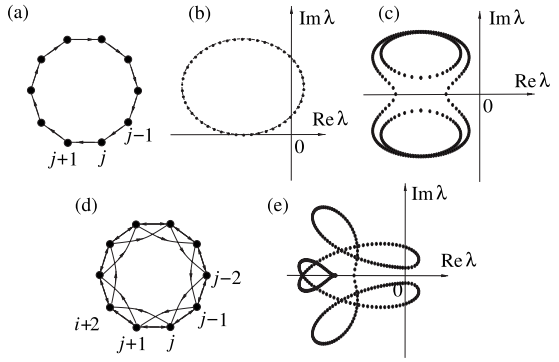

FIG. 1. (a) Ring of unidirectionally coupled oscillators. (b) Eigenvalues of the steady state for a ring of 50 unidirectionally coupled Stuart-Landau oscillators. (c) Eigenvalues for the ring of 150 oscillators determined by Eqs. (2) and (5). (d) More complicated network, corresponding to Eq. (2) with nonvanishing A and B_1 as in Eq. (5) and $B_{-1}=B_2=\mathrm{I}$, where I is the identity matrix. (e) Eigenvalues of the steady state for the network from (d).

rated, and the nonlinear functions H_j contain only terms of order 2 or higher and have the symmetry $H_j(u_1,\ldots,u_N)=H_{j+m}(u_{1+m},\ldots,u_N,u_1,\ldots,u_m)$. A and B_m are square matrices of size n, describing the linear part of the oscillator itself and of the coupling to the mth neighbor to the right, respectively. Following Ref. [27], we can write the linearized problem in a block diagonalized form,

$$\dot{\xi}_j = \left(A + \sum_m \gamma_j^m B_m\right)\xi_j, \tag{2}$$

where $\gamma_j=e^{2\pi i/Nj}$ for $j=1,\ldots,N$ are the eigenvalues of the $N\times N$ matrix

$$G = \begin{bmatrix} 0 & 1 & 0 & \cdots & 0 \\ 0 & 0 & 1 & \cdots & 0 \\ \cdot & \cdot & \cdot & \cdot & \cdot \\ 0 & \cdots & 0 & 0 & 1 \\ 1 & 0 & \cdots & 0 & 0 \end{bmatrix}.$$

Since the coupling to the mth neighbor is described by the coupling matrix G^m, the factor γ_j^m appears in Eq. (2). Note that we do not need here the condition $\Sigma_j G_{ij}=0$, which was used in Ref. [27] to distinguish between the synchronous mode and the asynchronous modes. From (2) we obtain immediately the characteristic equation in factorized form as

$$\chi(\lambda,j) := \det\left(\lambda\mathrm{I} - \mathrm{A} - \sum_m \gamma_j^m B_m\right) = 0, \tag{3}$$

where $j=1,\ldots,N$ and I is the identity matrix. At this moment, we introduce the limit of a large number of oscillators in the network. Using the fact that for $N\to\infty$ the roots of unity γ_j densely fill the unit circle in the complex plane, we replace the discrete family of network eigenvalues γ_j, $j=1,\ldots,N$, by the continuous family $e^{i\varphi}$, $\varphi\in(0,2\pi)$. In this way, we obtain from Eq. (3)

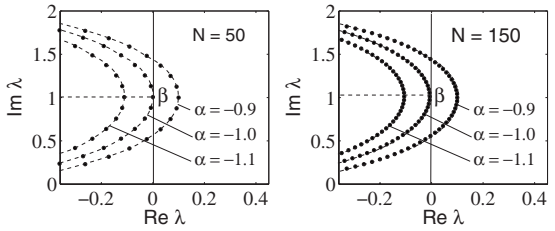

FIG. 2. Critical part of the spectrum for the stationary state of Eq. (6) with $\beta=1$ and changing α: stable ($\alpha=-1.1$), at bifurcation ($\alpha=-1$), and unstable ($\alpha=-0.9$). For increased N (right panel), the PCS curves (dashed lines) are unchanged, but more densely filled with eigenvalues.

$$\chi(\lambda,\varphi) := \det\left(\lambda\mathrm{I} - A - \sum_m e^{im\varphi} B_m\right) = 0 \tag{4}$$

for the location of the eigenvalues of the stationary state of the coupled system in the limit of $N\to\infty$. This equation is independent of the number of nodes N and determines n curves $\lambda(\varphi)$ in the complex plane, which become densely filled with eigenvalues for increasing N. We will call these curves the pseudocontinuous spectrum (PCS) in analogy to the pseudocontinuous spectrum of delay-differential equations with large delay [29]. Figure 1 shows some examples of networks and numerically computed eigenvalues where one can observe the curves of the PCS: for the unidirectionally coupled ring of Stuart-Landau oscillators [Fig. 1(a)] we obtain the spectrum [Fig. 1(b)], and for the coupling matrices

$$A = \begin{bmatrix} -2 & 1 \\ -1 & -1.5 \end{bmatrix}, \quad B_1 = \begin{bmatrix} -1 & 0.3 \\ -0.3 & 1 \end{bmatrix} \tag{5}$$

the spectrum of Fig. 1(c). For the more complicated network of Fig. 1(d) we obtain the spectrum of Fig. 1(e), using A and B_1 as above and additionally $B_{-1}=B_2=\mathrm{I}$.

The concept of the PCS allows the following main conclusions. (i) At a destabilization, the critical part of the spectrum is given by an arc of the PCS touching the imaginary axis (cf. Fig. 2). (ii) Since the PCS crossing the imaginary axis brings immediately a large number of eigenvalues to the right half plane, classical bifurcation theory is not suitable to describe the bifurcation scenario exhaustively. Instead, the destabilization in large coupled systems should be described in terms of instabilities of spatially extended systems [8,30–32], where eigenvalue (or gain) curves are typical [33,34].

The fact that the spectrum appears here for large N in the form of curves relies on the symmetry properties of the coupling structure. Indeed, the roots of unity γ_j are a representation of the underlying abstract symmetry group and, in the limit of $N\to\infty$, approximate the whole unit circle. Parametrizing this unit circle by the continuous parameter $\varphi\in(0,2\pi)$, we obtain the curves of the PCS, parametrized by φ too.

Note that the PCS can be calculated just by determining the roots of a polynomial of degree n, i.e., on the level of complexity of one single oscillator. Similarly, the above described condition for destabilization can be easily stated in

terms of this polynomial. As an example for this destabilization scenario, we study now in detail the behavior of a unidirectionally coupled ring of Stuart-Landau oscillators.

III. COUPLED STUART-LANDAU OSCILLATORS

Consider a unidirectionally coupled ring of Stuart-Landau oscillators [26],

$$\dot{z}_j = (\alpha + i\beta)z_j - z_j|z_j|^2 + e^{i\psi}z_{j+1} \tag{6}$$

with $j=1,\ldots,N$ and indices to be taken modulo N. Each individual oscillator, described by its complex amplitude z_j, follows the normal form of a supercritical Hopf bifurcation. Hence, without coupling, it undergoes a supercritical Hopf bifurcation governed by the real parameter α, where at $\alpha=0$ a stable limit cycle with frequency β emerges. We may rescale the coupling strength to unity such that there is as an additional parameter only the coupling phase ψ. Using the general formula (3), we obtain the eigenvalues of the steady state

$$\lambda_k = \alpha + i\beta + e^{i\psi_k}, \quad \psi_k := \psi + 2\pi k/N. \tag{7}$$

According to Eq. (4) the eigenvalues are located on a circle of PCS with the center at $\alpha+i\beta$ and radius 1 [cf. Fig. 1(b)]. Note that introducing a new continuous parameter is not necessary here since the coupling phase ψ already serves for this purpose and we will use the combined parameter ψ_k in the following. By increasing the control parameter α, the PCS shifts to the right and the steady state becomes unstable at $\alpha=-1$. Figure 2 shows the critical part of the spectrum, i.e., those eigenvalues that become unstable. Note that the destabilization threshold decreases from $\alpha=0$ for the uncoupled oscillators to $\alpha=-1$ for the coupled system.

IV. BIFURCATING MULTIPLE PERIODIC SOLUTIONS

We describe now the bifurcation scenario for increasing α. At $\alpha=-1$, the PCS crosses the imaginary axis (see Fig. 2) leading to a sequence of Hopf bifurcations. Due to the ring structure of the network, the bifurcating periodic solutions are rotating waves of the form $\bar{\mathbf{z}}=(\bar{z}_1,\ldots,\bar{z}_N)^T$, $\bar{z}_j = ae^{i(\omega t+j2\pi k/N)}$, where ω is the temporal frequency and each oscillator is phase shifted by $2\pi k/N$ with respect to the neighboring one. Substituting $\bar{\mathbf{z}}$ into Eq. (6), we obtain an equation for the unknown real parameters a and ω:

$$i\omega = \alpha + i\beta - a^2 + e^{i\psi_k},$$

which has N solutions,

$$a_k = \sqrt{\alpha + \cos\psi_k}, \tag{8}$$

$$\omega_k = \beta + \sin\psi_k, \quad k = 1,\ldots,N, \tag{9}$$

corresponding to periodic solutions

$$\bar{z}^{(k)} = a_k e^{i\omega_k t}[\gamma_k, \gamma_k^2, \ldots, \gamma_k^N]^T. \tag{10}$$

Each of them originates at a Hopf bifurcation at

$$\alpha_k = -\cos\psi_k, \tag{11}$$

where $a_k=0$. Figure 3(I) shows the amplitudes a_k of the bifurcating periodic solutions versus α. As for the single Stuart-Landau oscillator, the bifurcations are supercritical and the frequencies ω_k of the periodic solutions do not depend on α, leading to straight lines in the (ω,α) bifurcation diagram in Fig. 3(II). In this diagram, the periodic orbits appear along the circle

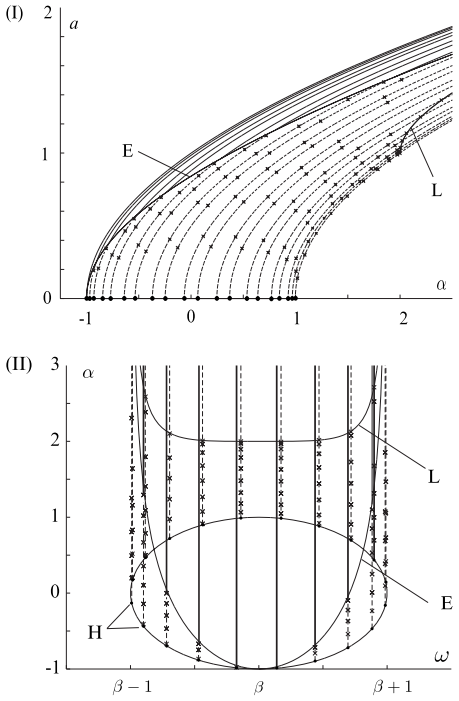

FIG. 3. Bifurcation diagram for 20 coupled Stuart-Landau oscillators: Amplitudes (I) and frequencies (II) versus parameter α. Branches of periodic solutions emerge unstable (dashed lines) at Hopf bifurcations (H), and undergo a sequence of torus bifurcations (crosses) until they are stable (bold lines) after the Eckhaus line (E).

$$\alpha^2 + (\omega - \beta)^2 = 1 \tag{12}$$

(line H).

V. STABILITY OF THE BIFURCATING PERIODIC SOLUTIONS

We investigate now the stability of the bifurcating periodic solutions (10). This can be performed analytically. We introduce new real variables x_j and y_j in Eq. (6) by

$$z_j = a_k\gamma_k^j e^{i\omega_k t}(x_j + iy_j).$$

With respect to the new variables, the system (6) has the form

$$\dot{x}_j = \alpha x_j - (\beta - \omega_k)y_j - a_k^2 x_j(x_j^2 + y_j^2) + x_{j+1}\cos\psi_k - y_{j+1}\sin\psi_k,$$

$$\dot{y}_j = \alpha y_j + (\beta - \omega_k)x_j - a_k^2 y_j(x_j^2 + y_j^2) + x_{j+1}\sin\psi_k + y_{j+1}\cos\psi_k. \tag{13}$$

Recall that the index $j=1,\ldots,N$ accounts for the number of the oscillator, whereas $k=1,\ldots,N$ refers to the correspond-

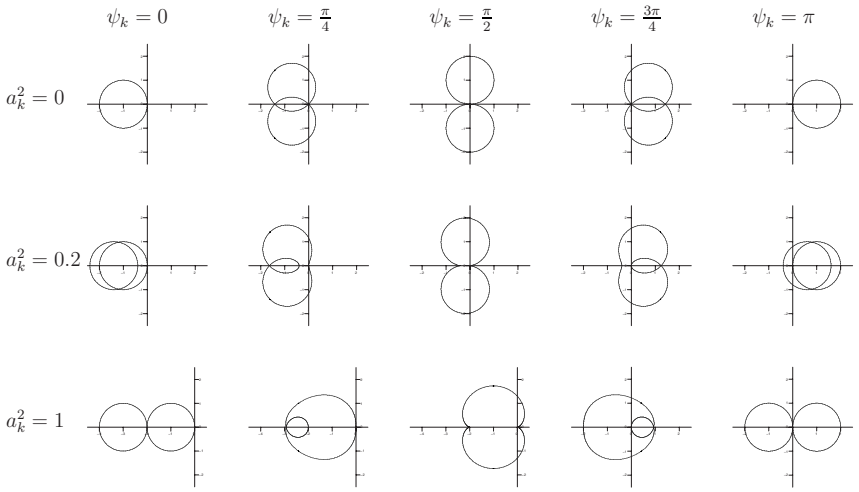

FIG. 4. Curves of pseudocontinuous Floquet spectrum for periodic orbits of Eq. (6) given by Eq. (16) for different amplitudes a_k and phase conditions ψ_k.

ing periodic solution under consideration. Indeed, for any fixed parameters α, β, and ψ_k, including a particular choice of k, the corresponding periodic solution (10) transforms into the stationary state

$$x_1 = \cdots = x_N = y_1 = \cdots = y_N = 1/\sqrt{2}$$

for the transformed system (13). Linearizing the system (13) around this stationary state, we obtain

$$\begin{bmatrix} (\delta x_j)' \\ (\delta y_j)' \end{bmatrix} = -\left(C_k + a_k^2 \begin{bmatrix} 1 & 1 \\ 1 & 1 \end{bmatrix} \right) \begin{bmatrix} \delta x_j \\ \delta y_j \end{bmatrix} + C_k \begin{bmatrix} \delta x_{j+1} \\ \delta y_{j+1} \end{bmatrix}, \tag{14}$$

where we defined

$$C_k := \begin{bmatrix} \cos\psi_k & -\sin\psi_k \\ \sin\psi_k & \cos\psi_k \end{bmatrix}$$

and used Eqs. (8) and (9) to eliminate α, β, and ω_k. Note that Eq. (14) has again the form of a unidirectionally coupled ring system. Therefore, we can use formula (3) to compute the eigenvalues. We obtain the characteristic equation

$$\det\left(\Lambda \mathrm{I} + a_k^2 \begin{bmatrix} 1 & 1 \\ 1 & 1 \end{bmatrix} + C_k(1-\gamma_l) \right) = 0,$$

which can be further reduced to the single complex equation

$$\Lambda^2 + 2\Lambda(a_k^2 + (1-\gamma_l)\cos\psi_k) + 2a_k^2(1-\gamma_l)\cos\psi_k + (1-\gamma_l)^2 = 0. \tag{15}$$

The quadratic equation (15) can be solved as

$$\Lambda_l^{\pm} = -a_k^2 - (1-\gamma_l)\cos\psi_k \pm \sqrt{a_k^4 + (1-\gamma_l)^2(\cos^2\psi_k - 1)}. \tag{16}$$

In this way, we have determined $2N$ Floquet exponents $\Lambda_l^{\pm}$, $l=1,\ldots,N$, of one particular periodic solution, given by a fixed choice of k. Similarly to the case of a steady state, the location of the Floquet exponents $\Lambda_l^{\pm}$ of a periodic solution is given by a pseudocontinuous spectrum $\Lambda^{\pm}(\varphi)$, which can be found from (15) by replacing again the family of network eigenvalues γ_l, $l=1,\ldots,N$, by the continuous family $e^{i\varphi}$ with the continuous parameter $\varphi \in (0, 2\pi)$:

$$\Lambda^{\pm}(\varphi) = -a_k^2 - (1-e^{i\varphi})\cos\psi_k \pm \sqrt{a_k^4 + (1-e^{i\varphi})^2(\cos^2\psi_k - 1)}. \tag{17}$$

In Fig. 4 we have plotted the curves $\Lambda^{\pm}(\varphi)$ for different values of ψ_k and a_k. Note that the curves for corresponding negative values of ψ_k are identical. One can observe that for $\cos\psi_k \leq 0$ the spectrum is unstable for all values of $a_k \geq 0$. For $\psi_k = 0$ the spectrum is stable. For other values of ψ_k with $\cos\psi_k > 0$ the periodic solution emerges unstable at the Hopf bifurcation, corresponding to $a_k = 0$, and eventually becomes stable (see also Fig. 3). Since the PCS is shifted to the left half plane it induces a sequence of torus bifurcations leading finally to stabilization. Even though in the limit $N \to \infty$ the PCS will become densely filled with eigenvalues and the number of these torus bifurcations grows unboundedly, the location of the final stabilization can be determined in an asymptotic manner by studying the shape of the PCS. Since a periodic solution always has a zero Floquet exponent, the curves $\Lambda^{\pm}(\varphi)$ have to pass through the origin. Indeed, from Eq. (16) we obtain that $\Lambda^{+}(0) = 0$. The stabilization takes place by the curve $\Lambda(\varphi)$ changing at $\varphi = 0$ from positive to negative curvature (this scenario is well known as a modulational instability in spatially extended systems [35]). Therefore, the condition for the stability boundary can be written as

$$\left. \frac{\partial^2 \Gamma}{\partial^2 \Omega} \right|_{\varphi=0} = 0, \tag{18}$$

$$\left. \frac{\partial \Omega}{\partial \varphi} \right|_{\varphi=0} \neq 0, \tag{19}$$

where $\Lambda^{+} = \Gamma + i\Omega$. Equations (18) and (19) imply that the curve $\Gamma(\Omega)$ touches the imaginary axis with zero curvature at the origin. Note that the second condition is necessary to make sure that the curve is locally a graph over the imaginary axis. Differentiating Eq. (17), we obtain

$$\frac{\partial \Lambda^{+}(0)}{\partial \varphi} = i \cos \psi_k \tag{20}$$

and observe that Eq. (19) is satisfied in the region we are interested in. Since moreover

$$\frac{\partial \Gamma(0)}{\partial \varphi} = 0,$$

it follows that Eq. (18) is equivalent to

$$\frac{\partial^2 \Gamma(0)}{\partial^2 \varphi} = 0,$$

and we obtain from differentiating Eq. (17) twice the final condition

$$\frac{\partial^2 \Gamma(0)}{\partial^2 \varphi} = \frac{1 - \cos^2 \psi_k}{a_k^2} - \cos \psi_k = 0. \tag{21}$$

In order to come back to the original bifurcation parameter α, we use Eq. (8) to obtain from Eq. (21) the expression

$$a_k^2 = \frac{3\alpha}{4} + \sqrt{\left(\frac{\alpha}{4}\right)^2 + \frac{1}{2}}, \tag{22}$$

which for $\alpha \geq -1$ describes the curve E in Fig. 3(I). Using additionally Eq. (9) and regarding $\cos \psi_k > 0$, we can also eliminate a_k and obtain the expression

$$\alpha = \frac{2(\omega - \beta)^2 - 1}{\sqrt{1 - (\omega - \beta)^2}} \tag{23}$$

for the curve E in Fig. 3(II).

The complete bifurcation scenario for $N=20$ is illustrated in Fig. 3. We have chosen here $\psi=0.14$. Figure 3(I) shows the amplitudes (8) and Fig. 3(II) the frequencies of all branches of periodic solutions versus the bifurcation parameter α. According to Eq. (11), the solution with ψ_k closest to zero, and hence frequency closest to β, bifurcates first for increasing α. It emerges as stable and remains stable as α increases further [cf. Eq.(16) and Fig. 4]. In our case, this orbit corresponds to $k=0$, with $\psi_0=0.14$, $\alpha_0 \approx -0.99$, and $\omega_0 \approx \beta + 0.14$. Next, the periodic solution with $k=-1$ bifurcates at $\alpha_{-1} \approx -0.985$, which corresponds to $\psi_{-1} \approx -0.17$ and temporal frequency $\omega_{-1} \approx 0.83$. It is then followed by the solution with $k=1$, and so on. All solutions with $k \neq 0$ emerge as unstable and gain stability after a sequence of torus bifurcations. The location of the torus bifurcations (crosses) for fixed $N=20$ has been obtained numerically by solving for pure imaginary solutions of Eq. (16). For further periodic solutions with increasing k, the number of torus bifurcations needed to gain stability increases. At the same time, the frequency offset increases up to ± 1. One can observe that the last of these torus bifurcations is well approximated by the asymptotic formulas (22) and (23) in Figs. 3(I) and 3(II), respectively. A stabilization takes place only for the periodic solutions with $\cos \psi_k > 0$, i.e., here $|k| < 5$. All other periodic solutions stay unstable for all values of α. This can be seen from Eqs. (20) and (21), which imply that $\Gamma(\Omega)$ has a positive curvature at $\varphi=0$ when $\cos \psi_k < 0$. In particular, the solution with $k=\frac{N}{2}$, corresponding to an antiphase

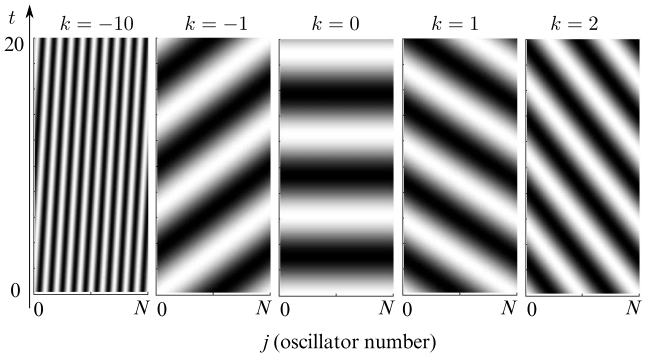

FIG. 5. Bifurcation scenario independent of the number of the network nodes. *H*, multiple branches of periodic solutions appear at Hopf bifurcations. *E*, Eckhaus line, at which these periodic orbits become stable. Gray, region of existence of periodic orbits. Dark gray, stability region. Hatched, region of torus bifurcations.

synchronization of subsequent oscillators, is unstable, while its frequency is again close to β. A similar phenomenon has been observed in the Lang-Kobayashi model for semiconductor lasers with delayed optical feedback. There, the possibly stable and unstable rotating wave solutions were called *modes* and *antimodes*, respectively. In Fig. 3 one can observe that there are also torus bifurcations for periodic solutions with $\cos \psi_k < 0$. The curve describing the region in parameter space for these torus bifurcations can be found by looking for a second branch of the PCS, touching the imaginary axis at zero. Indeed, choosing $\varphi=\pi$ and inserting $\Lambda=0$ into Eq. (15) gives

$$a_k^2 \cos \psi_k = -1. \tag{24}$$

Using Eqs. (8) and (9) we obtain the equations

$$a_k^2 = \frac{\alpha}{2} + \sqrt{\frac{\alpha^2}{4} - 1}, \tag{25}$$

$$(\beta - \omega_k)^2 = 2 - \frac{\alpha^2}{2} + \alpha \sqrt{\frac{\alpha^2}{4} - 1}. \tag{26}$$

for the curve L in Figs. 3 and 6. Note that these curves are valid exactly in the case of even N, where $\varphi=\pi$ holds true for $l=N/2$, and valid only in an asymptotic sense for large N, otherwise.

Since the spectrum (16) depends only on the combined parameter $\psi_k = \psi + 2k\pi/N$, a value $\psi \neq 0$ leads only to a shift of the wave number k for corresponding periodic solutions. Choosing k such that ψ_k is closest to zero, we obtain the primary periodic solution, which bifurcates first, is always stable, and has the frequency closest to β. For the other periodic solutions with different stability properties as described above, the wave number is shifted accordingly. In particular, for $\psi=\pi$ the solution with anti-phase-synchronized neighboring oscillators is the most stable one. Under a continuous change of ψ, a periodic solution with fixed k changes its stability properties again in torus bifurcations.

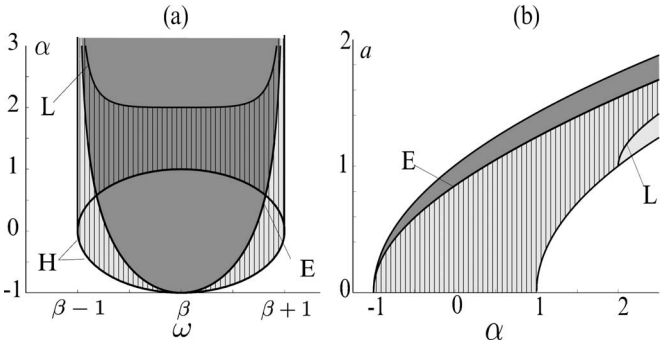

FIG. 6. Spatial patterns for some of the bifurcating time-periodic solutions (10) corresponding to different values of k. Note that the solutions with $k=1$ and -1 have different temporal frequencies.

For an increasing number of oscillators, the main features of this complex bifurcation scenario remain unchanged: the conditions determining the existence region of periodic solutions do not depend on N and at the Hopf curve (11) an increasing number of branches of periodic solutions appears, densely filling the frequency band between $\beta-1$ and $\beta+1$. For $\cos\psi_k>0$ there is a region of stability given by the asymptotic stability boundary (22) or (23). Figure 6 shows that those with the highest amplitudes [Fig. 6(b)] and frequency closest to β [Fig. 6(a)] are stable. The region of unstable modes with $\cos\psi_k>0$ becomes densely filled with torus bifurcations and there is a similar region for $\cos\psi_k<0$, enclosed by the curve L given by Eqs. (25) and (26).

The bifurcation scenario resembles the essential features of the classical Eckhaus scenario for PDEs of reaction-diffusion type [28]. There in a similar way a spatially homogeneous stationary state becomes unstable with respect to a growing band of spatial wave numbers, and the regions of existence and stability of the bifurcating spatially periodic solutions (Turing patterns [32]) are given by parabolas. These parabolas coincide in leading order with the curves given by Eqs. (12) and (23), respectively. Moreover, in the case of PDEs with periodic boundary conditions one observes discrete spatial modes, interchanging their stability in a similar way in torus bifurcations while their number increases with the size of the domain (see Ref. [36]). This suggests in particular that for large N and α close to -1 a description by an amplitude equation of Ginzburg-Landau type should be possible. A major difference of the ring of coupled oscillators from the classical scenario is that the bifurcating solutions are not stationary patterns, but time-periodic rotating waves with a nontrivial dependence of the temporal frequency from the wave number given by Eq. (9); see also Fig. 5. Furthermore, it is remarkable that such diffusive patterns appear here in a system with purely unidirectional, i.e., convective coupling. Finally, we want to point out that in our example of the coupled Stuart-Landau oscillators, we obtain a complete and global description of the bifurcation, including expressions for the global stability boundaries.

VI. CONCLUSIONS

This paper reveals a mechanism for the destabilization of large oscillator lattices with cyclic symmetry. First, we show how to calculate efficiently the spectrum in a large lattice, and characterize the spectral situation leading to the described destabilization phenomenon. Then we use the Stuart-Landau oscillator as an example to study the scenario in detail. Based on our analysis, the following main conclusions can be drawn. (i) For identical oscillators with a fixed intrinsic frequency, in a large lattice this frequency can split up into a quasicontinuous frequency band of periodic solutions. (ii) The different frequencies come along with spatial patterns of different periods. (iii) Among this quasicontinuum of available periodic states, there is a competition-cooperation mechanism with a universal stability boundary which can be understood in analogy to the well-known Eckhaus scenario.

[1] S. H. Strogatz, Nature (London) **410**, 268 (2001).
[2] R. Zillmer, R. Livi, A. Politi, and A. Torcini, Phys. Rev. E **74**, 036203 (2006).
[3] E. Mosekilde, Y. Maistrenko, and D. Postnov, *Chaotic Synchronization: Application to Living Systems* (World Scientific, Singapore, 2002).
[4] A. Pikovsky, M. Rosenblum, and J. Kurths, *Synchronization: A Universal Concept in Nonlinear Sciences* (Cambridge University Press, Cambridge, U.K., 2001).
[5] *Analysis, Modeling and Simulation of Multiscale Problems*, edited by A. Mielke (Springer, Heidelberg, 2006).
[6] R. E. Mirollo and S. H. Strogatz, Physica D **205**, 249 (2005).
[7] O. Rudzick and A. Pikovsky, Phys. Rev. E **54**, 5107 (1996).
[8] D. E. Postnov, O. V. Sosnovtseva, and E. Mosekilde, Chaos **15**, 013704 (2005).
[9] P. G. Lind, J. Corte-Real, and J. A. C. Gallas, Phys. Rev. E **69**, 066206 (2004).
[10] J. Jost and M. P. Joy, Phys. Rev. E **65**, 016201 (2001).
[11] V. A. Makarov, E. del Río, W. Ebeling, and M. G. Velarde, Phys. Rev. E **64**, 036601 (2001).
[12] A. M. Morgante, M. Johansson, G. Kopidakis, and S. Aubry, Phys. Rev. Lett. **85**, 550 (2000).
[13] A. Giacometti, M. Rossi, and L. Battiston, Phys. Rev. E **73**, 036214 (2006).
[14] L. Pecora, T. Carroll, G. Johnson, D. Mar, and J. Heagy, Chaos **7**, 520 (1997).
[15] S. Yanchuk, Y. Maistrenko, and E. Mosekilde, Physica D **154**, 26 (2001).
[16] S. Yanchuk, Y. Maistrenko, and E. Mosekilde, Chaos **13**, 388 (2003).
[17] L. M. Pecora and T. L. Carroll, Phys. Rev. Lett. **64**, 821 (1990).
[18] Y. Kuramoto, in *International Symposium on Mathematical Problems in Theoretical Physics,* edited by H. Araki, Lecture Notes in Physics Vol. 30 (Springer, New York, 1975), p. 420.

[19] A. Takamatsu, R. Tanaka, H. Yamada, T. Nakagaki, T. Fujii, and I. Endo, Phys. Rev. Lett. **87**, 078102 (2001).
[20] P. Woafo and H. G. Enjieu Kadji, Phys. Rev. E **69**, 046206 (2004).
[21] I. Waller and R. Kapral, Phys. Rev. A **30**, 2047 (1984).
[22] H. Daido, Phys. Rev. Lett. **78**, 1683 (1997).
[23] J. G. Restrepo, E. Ott, and B. R. Hunt, Phys. Rev. Lett. **93**, 114101 (2004).
[24] D. M. Abrams and S. H. Strogatz, Phys. Rev. Lett. **93**, 174102 (2004).
[25] P. C. Bressloff, S. Coombes, and B. de Souza, Phys. Rev. Lett. **79**, 2791 (1997).
[26] Y. Kuramoto, *Chemical Oscillations, Waves, and Turbulence* (Springer, Berlin, 1984).
[27] L. M. Pecora and T. L. Carroll, Phys. Rev. Lett. **80**, 2109 (1998).
[28] W. Eckhaus, *Studies in Non-Linear Stability Theory*, Springer Tracts in Natural Philosophy (Springer, Berlin, 1965).
[29] M. Wolfrum and S. Yanchuk, Phys. Rev. Lett. **96**, 220201 (2006).
[30] P. Manneville, *Dissipative Structures and Weak Turbulence* (Academic Press, San Diego, 1990).
[31] A. C. Newell, T. Passot, and J. Lega, Annu. Rev. Fluid Mech. **25**, 399 (1993).
[32] P. Borckmans, G. Dewel, A. D. Wit, and D. Walgraef, *Chemical Waves and Patterns* (Kluwer Academic, Dordrecht, 1995), pp. 323–363.
[33] A. R. Hutson and D. L. White, J. Appl. Phys. **33**, 40 (1962).
[34] S. P. Kuznetsov, E. Mosekilde, G. Dewel, and P. Borckmans, J. Chem. Phys. **106**, 7609 (1997).
[35] M. C. Cross and P. C. Hohenberg, Rev. Mod. Phys. **65**, 851 (1993).
[36] L. S. Tuckerman and D. Barkley, Physica D **46**, 57 (1990).